ACS APPLIED MATERIALS & INTERFACES

Research Article

www.acsami.org

Yolk–Shell Upconversion Nanocomposites for LRET Sensing of Cysteine/Homocysteine

Lingzhi Zhao, Juanjuan Peng, Min Chen, Yi Liu, Liming Yao, Wei Feng,* and Fuyou Li*

Department of Chemistry & The State Key Laboratory of Molecular Engineering of Polymers & Institute of Biomedicine Science, Fudan University, Shanghai 200433, P. R. China

Supporting Information

ABSTRACT: The fabrication of lanthanide upconversion nanocomposites as probes has become a new research hotspot due to its special advantages via utilizing upconversion luminescence (UCL) as a detection signal. Herein, a hybrid organic dye modified upconversion nanophosphor is successfully developed as a nanoprobe for cysteine/homocysteine. Yolk–shell structured upconversion nanoparticles (YSUCNP) with lanthanide upconversion nanophosphor as moveable core and silica as mesoporous shell are synthesized, and a colorimetric chemodosimeter for cysteine/homocysteine is accommodated in the hollow cavities. Thus, cysteine/homocysteine can be quantitatively detected on the basis of luminescent resonance energy transfer (LRET) in a UCL turn-off pattern. The dye-loaded YSUCNP possess good dispersibility in aqueous solution; thus detection of the targeted molecule can be achieved in pure water. Cellular experiments carried out with laser-scanning upconversion luminescence microscopy further demonstrate that the dye-loaded YSUCNP can serve as an intracellular nanoprobe to detect cysteine/homocysteine. Moreover, this dye-loading protocol can be developed as a common approach to construct other chemodosimeter-modified UCNP hybrid nanoprobes, as proved by a UCL turn-on style sensor for cyanide.

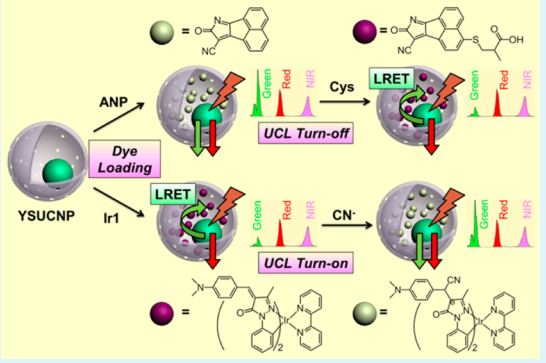

KEYWORDS: *upconverting luminescence, chemodosimeter, LRET, cysteine, homocysteine*

INTRODUCTION

With the unique ability to convert long-wavelength near-infrared (NIR) light to short-wavelength light, lanthanide upconversion nanophosphors (UCNP) have been considered as a promising class of luminescent labels.[1−8] In contrast to conventional fluorescence probes, UCNP feature several attractive optical properties, such as a narrow emission band, high photostability, no blinking, and no autofluorescence from biosamples,[9−18] which affords the UCNP great potential in sensing for in vivo samples.[19−25]

Because UCNP generally lack a recognition moiety, a special recognition group must be conjugated with UCNP to realize sensing functionalization with upconversion luminescence (UCL) as detection signal. To tune the UCL intensity in the presence of the analyte, a chromophore as the energy acceptor is usually introduced into UCNP to achieve luminescence resonance energy transfer (LRET)[26] from the UCNP (donor) to the chromophore (acceptor). To date, several upconversion LRET (UC-LRET) nanosystems have been developed for detection of biomacromolecules (such as DNA,[27−29] metalloproteinase,[30] avidin,[31] and thrombin[32,33]), metal cations, anions and oxygen,[34−39] in which the energy transfer process is utilized to modulate the UCL intensity. However, no UCL-based nanoprobe has been reported to detect amino acids.

Homocysteine (Hcy) and cysteine (Cys) play crucial roles in biological systems. The level of Hcy in plasma is an indicator of disorders including cardiovascular and Alzheimer's disease.[40] Cys deficiency is related to slowed growth, edema, lethargy, liver damage, muscle and fat loss, skin lesions, and weakness.[41] The detection of Hcy and Cys has attracted increasing attention in recent years. Unfortunately, there is no example of UCNP for detection of Hcy and Cys, although there are many organic fluorescence probes for the specific detection of Hcy and Cys with the help of organic solvent.[42−53]

We are interested in developing a UCL-based nanoprobe for the highly selective detection of Cys/Hcy over other amino acids. In this present study, we fabricated upconversion nanocomposites by simply loading 8-oxo-8H-acenaphtho[1,2-*b*]pyrrole-9-carbonitrile (ANP, as colorimetric chemodosimeter of Cys/Hcy, Scheme 1)[47]into a yolk–shell upconverting nanophosphor (YSUCNP, Scheme 1) for UC-LRET detection of Cys/Hcy in aqueous solution. Herein, the as-prepared nanosystem was denoted as YSUCNP-ANP. In the presence of Cys/Hcy, color of YSUCNP-ANP changed from yellowish to purple, and green UCL emission decreased concomitantly, that is, YSUCNP-ANP was a UCL turn-off nanoprobe for Cys/Hcy. Importantly, because of the hollow nanostructure and high loading efficiency of hydrophobic compounds for YSUCNP,

Received: March 1, 2014
Accepted: April 8, 2014
Published: April 8, 2014

Scheme 1. Schemetic Illustration of the Yolk−Shell Upconverting Nanophosphors Loaded with Some Chromophoric Chemodosimeters to Construct UC-LRET probes for Cys/Hcy or CN^-[a]

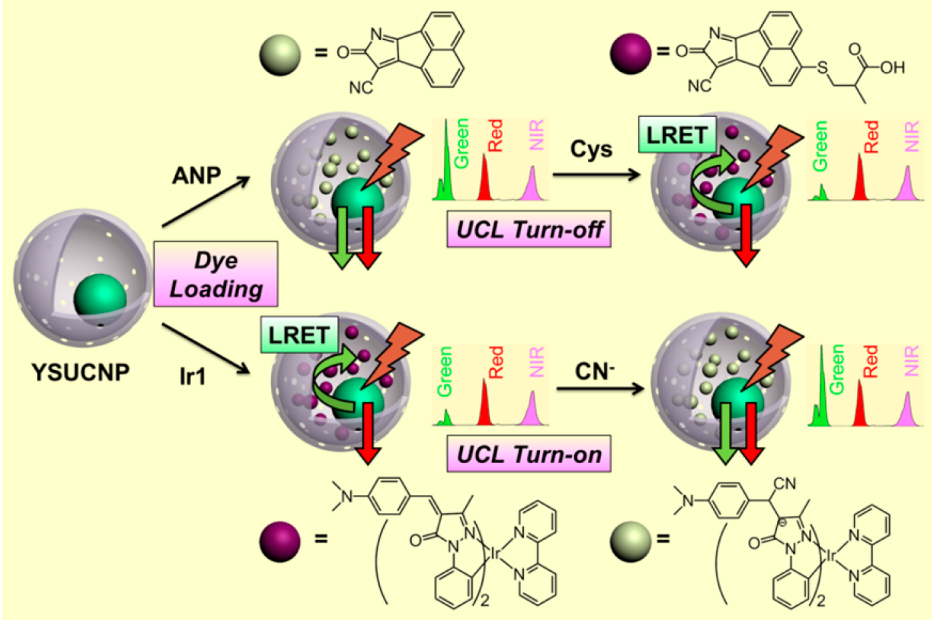

[a]The UC-LRET process from the UCNP (donor) to the chromophoric chemodosimeters (acceptor), turn-on and turn-off of the UCL emission in green region was separately adopted to realize ratiometric detection of the special analytes.

such design strategy could be extended to detect other analytes. For example, the iridium(III) complex[54] (Ir1, Scheme 1) as CN^--sensitive chemodosimeter could be loaded into the hollow space of YSUCNP to construct a proof-of-concept of turn-on style UC-LRET nanoprobe.

RESULTS AND DISCUSSION

1. Design of the UCNP-Based LRET Probe. Scheme 1 shows the design strategy of the UCL probe based on LRET process between the UCNP and the loaded chromophoric chemodosimeter. Herein, to achieve the ratiometric UCL detection, UCNP with a composition of $NaLuF_4$ codoped with 20% of Yb^{3+}, 1% of Er^{3+}, and 0.5% of Tm^{3+} (denoted as $NaLuF_4$:Yb,Er,Tm) showing both UCL emission at 800 and 540 nm were synthesized as energy donor. To tune the UCL intensity, two chromophoric chemodosimeters or their sensing products were introduced as energy acceptors. Importantly, in order to gather the chromophoric chemodosimeters or their products around the UCNP, a yolk−shell nanostructure was fabricated, and the hollow cavities of the YSUCNP were utilized to accommodate the chromophoric chemodosimeters as guest molecules. Such strategy do not require any specific chemical modifications to the probe molecule, which was distinguished from the previous method.[54,55] Moreover, the chemodosimeter-loaded YSUCNP with hydrophilic silica shell as outer layer was allowed to disperse in aqueous solutions to make the detection system workable in pure aqueous solution.

To obtain a UC-LRET-based sensor, overlap between the adsorption spectra of the chemodosimeters (or their products) and the emission spectrum of UCNP is necessary. In our design strategy, the intense green UCL of Er^{3+}-doped UCNP was adopted as the responsive signal. The reaction of the targeted molecule and chemodosimeter could change the adsorption band of the loaded chemodosimeters, and further influence the green UCL intensity to accomplish detection of the analyte (Scheme 1). According to these criteria, two kinds of organic probes, ANP[47] and Ir1,[54] were selected to modulate the energy transfer between UCNP and chromophoric chemodosimeters. Herein, ANP-loaded YSUCNP and Ir1-loaded YSUCNP were abbreviated as YSUCNP-ANP and YSUCNP-Ir1, respectively.

2. Characterizations of YSUCNP. The TEM images of the $NaLuF_4$:Yb,Er,Tm cores and the yolk−shell structured nanoparticle YSUCNP are shown in Figure 1. The $NaLuF_4$:Yb,Er,Tm nanocrystals possess a uniform size of ∼28 nm (Figure 1a) and show the β-phase, which was confirmed by XRD pattern (Figure 2a).

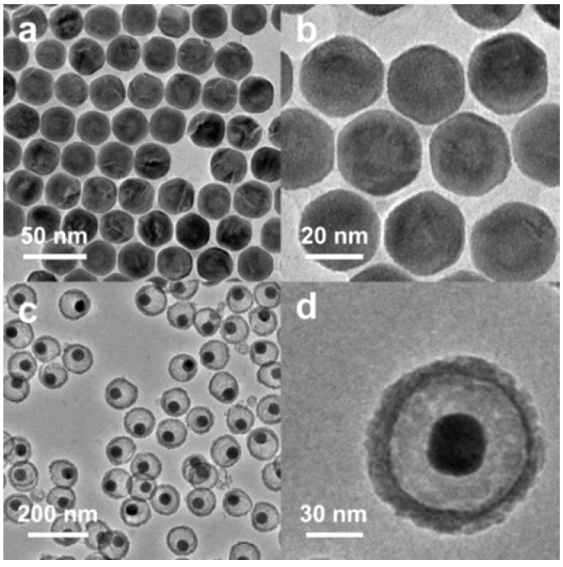

Figure 1. TEM images of (a, b) UCNP $NaLuF_4$:Yb,Er,Tm nanocrystals and (c, d) YSUCNP nanoparticles.

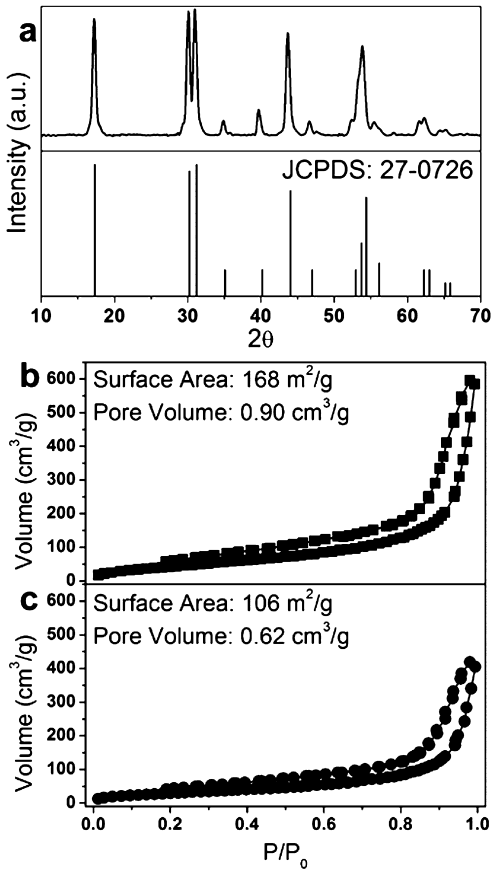

Figure 2. (a) XRD pattern of $NaLuF_4$:Yb,Er,Tm nanoparticles, and the standard XRD pattern is from Joint Committee for Powder Diffraction Studies (JCPDS) card 27−0726. (b, c) Nitrogen adsorption−desorption isotherms of the (b) YSUCNP and (c) YSUCNP-ANP.

A modified sol−gel method using mixed surfactant as a template[53,54] was introduced to coat a hollow silica shell onto each $NaLuF_4$:Yb,Er,Tm nanocrystal. The final yolk−shell structured nanoparticles (YSUCNP) were formed by removal of the surfactant template by extraction. The YSUCNP obtained were uniform nanospheres with an average diameter of 90 nm (Figure 1c), and the thickness of the silica shell layer was measured to be ∼10 nm from the TEM image (Figure 1d). Nitrogen adsorption−desorption isotherm of YSUCNP is shown in Figure 2b. The yolk−shell structured YSUCNP possess a surface area of 168 $cm^2\ g^{-1}$ and a large pore volume of 0.90 $cm^3\ g^{-1}$, which provides YSUCNP with the ability to accommodate guest molecules inside its hollow cavities.[56]

The organic colorant chemodosimeters[47] were loaded into the hollow cavities of YSUCNP through the physical adsorption method to form the chemodosimeter-loaded nanostructure YSUCNP-ANP. From the N_2 adsorption−desorption isotherm of YSUCNP-ANP (Figure 2c), it can be deduced that the surface area and pore volume of YSUCNP were decreased by ∼30% after the loading of ANP (106 $cm^2\ g^{-1}$ and 0.62 $cm^3\ g^{-1}$, respectively). The reduction of surface area and pore volume confirmed that the chemodosimeters were loaded inside the hollow cavities, rather than adsorbed onto the outer surface or simply mixed with YSUCNP.

3. UCL Sensing of Cys/Hcy by YSUCNP-ANP. Considering the fact that ANP could react with Cys/Hcy to form a new compound with an appearance of the new absorption band at 550 nm,[47] it is reasoned that the nanostructure YSUCNP-ANP can be interacted with Cys/Hcy. Herein, the interaction of YSUCNP-ANP with Cys was investigated in detail. The absorption spectra of YSUCNP-ANP, YSUCNP-ANP reacted with Cys, and the UCL spectrum of YSUCNP are shown in Figure 3. No obvious absorption of ANP in the visible

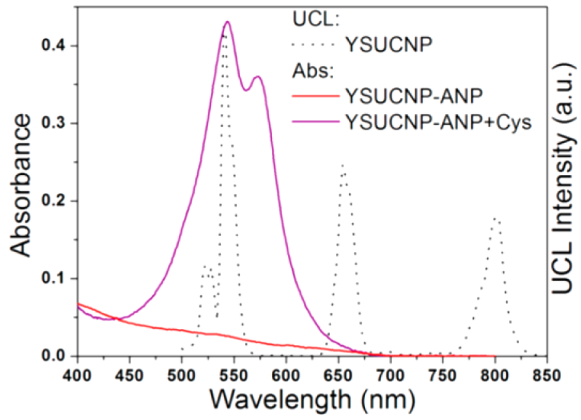

Figure 3. UV−vis absorption spectra of YSUCNP-ANP (red line), YSUCNP-ANP upon addition of Cys (purple line) and the UCL spectrum of YSUCNP (dot line).

wavelength range is apparent. Upon addition of Cys, ANP-Cys were formed with a new adsorption band from 428 to 680 nm with two peaks at 544 and 572 nm,[57] which overlapped with the green UCL emissions corresponding to $^2H_{11/2} \rightarrow {}^4I_{15/2}$ transition at 522, 528 nm and $^4S_{3/2} \rightarrow {}^4I_{15/2}$ transition at 540 nm of Er^{3+}. This spectral change will launch the LRET process from the UCL emission of YSUCNP to the absorption band of ANP-Cys addition product, with resulting turn-off of the green UCL. Therefore, ratiometric detection of Cys was successfully achieved by using the UCL emission at 800 nm ($^3H_4 \rightarrow {}^3H_6$ transition of Tm^{3+}) as internal reference.

The detailed upconversion sensing experiments for Cys were carried out in aqueous solution. YSUCNP-ANP with an ANP loading ratio of 483 μmol/g was dispersed in PBS (pH 7.3) to achieve a concentration of 50 μM for ANP. Upon addition of Cys, the color of YSUCNP-ANP changed from yellowish to purple (inset of Figure 4a), meanwhile the UCL intensity at 540 nm ($^4S_{3/2} \rightarrow {}^4I_{15/2}$ transition) decreased concomitantly, indicating a UCL turn-off style sensor for Cys was successfully constructed. From the optical images of YSUCNP-ANP before and after the addition of 50 equiv. of Cys (taken with a 540 ± 10 nm band-pass filter), the change in green UCL emission could be intuitively observed. Figure 4a shows the detailed UCL titration spectra of YSUCNP-ANP suspension with various equivalents (eq) of Cys (0−50 equiv). The ratio of the UCL intensity at 540 to 800 nm (UCL_{540}/UCL_{800}) decreased with the addition of Cys in the range of 0−18 eq., which showed fine linearity (inset of Figure 4b), implying the capability of quantitative Cys sensing with YSUCNP-ANP. The curve then inflected at 18 eq.; the slope was significantly reduced between 18 and 50 equiv. (Figure 4b). The detection limit for Cys was calculated to be 28.5 μM. Moreover, as another amino acid homocysteine (Hcy) also contains a thiolgroup, YSUCNP-ANP could respond toward Hcy in aqueous solution. The UCL_{540}/UCL_{800} value for YSUCNP-ANP upon addition of different equivalents of Hcy is shown in Figure S1 in the Supporting Information. The linear relation of

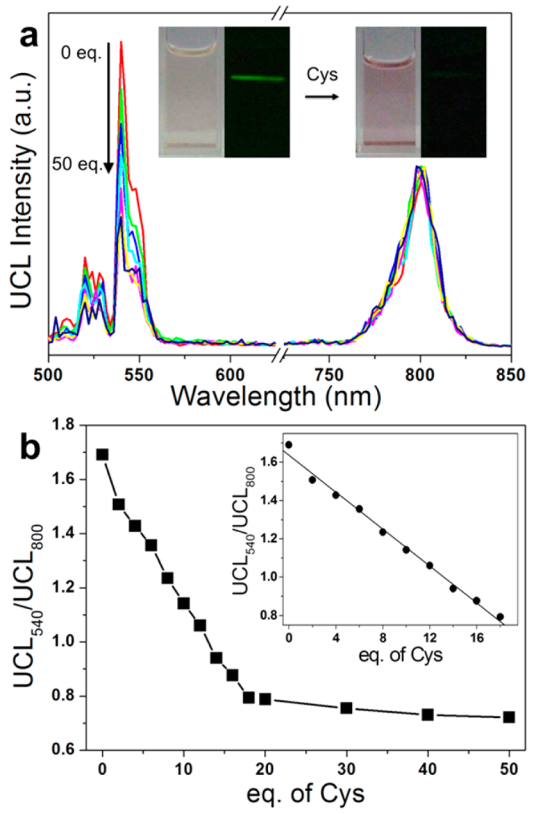

Figure 4. UCL sensing of Cys by YSUCNP-ANP. (a) UCL spectra of 50 μM YSUCNP-ANP in PBS (pH 7.5) upon addition of Cys. Inset: the change in photographs of bright-field and UCL emission of YSUCNP-ANP in the absence or presence of Cys. (b) Ratio of UCL intensities at 540 and 800 nm (UCL_{540}/UCL_{800}) for YSUCNP-ANP upon addition of different equivalent of Cys. Inset: the linear fitting of UCL_{540}/UCL_{800} in the linearity range.

the titration curve for Hcy was similar to Cys, implying good reproducibility of the method. The contribution of reabsorption for the quenching of 540 nm upconversion luminescence is estimated to be 5% using YSUCNP and free ANP as the control experiment.

4. Selectivity UCL Tests of YSUCNP-ANP. The selective response of YSUCNP-ANP to different amino acids, thiol-bearing peptide glutathione (Glu) and protein BSA with Cys residues was also studied in PBS solution (pH 7.3). As shown in Figure 5a, neither obvious change for the UCL_{540}/UCL_{800} value nor the color of the 50 μM YSUCNP-ANP suspension can be observed upon addition of 2 mM natural amino acids: alanine (Ala), tryptophan (Try), arginine (Arg), isoleucine (Iso), Asparticacid (Asp), serine (Ser), glycine (Gly), valine (Val), leucine (Leu), asparagine (Asn), tyrosine (Tyr), methionine (Met), proline (Pro), lysine (Lys), threonine (Thr), and histidine (His) without thiol groups and glutathione (Glu), or 2 mg/mL biomarcomolecule of BSA. It is worth noting that while ANP could slowly respond toward Glu in methanol/HEPES solution (7:3, v/v, pH 7),[47] the nanosensing system also showed no response to Glu in PBS even after 24 h. This can be attributed to the reduced reaction activity of the thiol group in Glu in aqueous phase. The fact indicated that our this designed nanosystem YSUCNP-ANP provided a new strategy of improving selectivity of Cys/Hcy over than other amino acids.

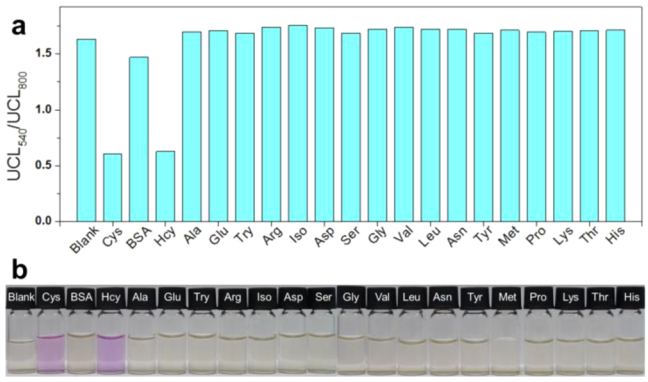

Figure 5. (a) Ratiometric UCL intensity (UCL_{540}/UCL_{800}) for YSUCNP-ANP (50 μM for ANP concentration) in PBS solution (pH 7.5) upon addition of 2 mM of different amino acids and 2 mg/mL BSA after 24 h. (b) Photos of color changes of the YSUCNP-ANP upon addition of different amino acids, Glu or BSA.

5. UCL Monitoring of Intracellular Cys/Hcy by YSUCNP-ANP. To assess the capability of YSUCNP-ANP for monitoring intracellular Cys/Hcy, laser-scanning upconversion luminescence microscopy (LSUCLM) was employed to image KB cellsincubated with YSUCNP-ANP (Figure 6a–c). Moreover, in the control group, the KB cells were initially pretreated with 200 μM thiol-reactive agent N-ethylmaleimide (NEM) at 37 °C for 30 min to form the absence of Cys/Hcy in the cells, before the incubation of YSUCNP-ANP (Figure 6d–f). Under CW 980 nm excitation, the UCL emissions detected at 515–560 nm (green region) and 635–680 nm (red region) were separately collected. As shown in Figure 6a, the green UCL from the KB cells treated only by YSUCNP-ANP (42 $\mu g\ mL^{-1}$, 20 μM of loaded ANP) was relatively weak, whereas the green UCL from the NEM-treated cells was much more intense (Figure 6d). Furthermore, the ratiometric UCL imaging of the YSUCNP-ANP-incubated KB cell pretreated with or without NEM was compared, using ratio of green UCL intensity to red one as detection signal. As shown in images c and f in Figure 6, an obvious red UCL signal and a relative weak ratio of green/red UCL can be clearly observed for the YSUCNP-ANP-incubated KB cells without the treatment of NEM, indicating YSUCNPs-ANP could interact with intracellular Cys/Hcy. Moreover, the measured UCL spectra (Figure 6g) further proved that the green UCL of YSUCNP-ANP was quenched upon treatment with intracellular Cys/Hcy. These facts confirmed that the YSUCNP-ANP can be successfully applied as a ratiometric UCL nanoprobe to indicate thiol-bearing amino acids in living cells.

6. Demonstration of the Universality of the Upconversion Nanoprobe Based on YSUCNP. As the hollow cavities of YSUCNP can indiscriminately accommodate guest molecules, this approach can also be extended as a general method to construct UC-LRET-based nanocomposites by simply loading other chemodosimeters in YSUCNP. Another UCL turn-on style sensor was demonstrated here to prove the universality of the method.

By adopting the chromophoric complex Ir1 (Scheme 1) as the energy acceptor into the YSUCNPs, a similar UC-LRET nanoprobeYSUCNP-Ir1 can be constructed. The chemodosimeter Ir1 with a strong adsorption band at 527 nm can effectively quench the green UCL emission of YSUCNP after being loaded (Figure 7a). CN^- can be added to react with the α,β-unsaturated carbonyl moiety of Ir1 to reduce the

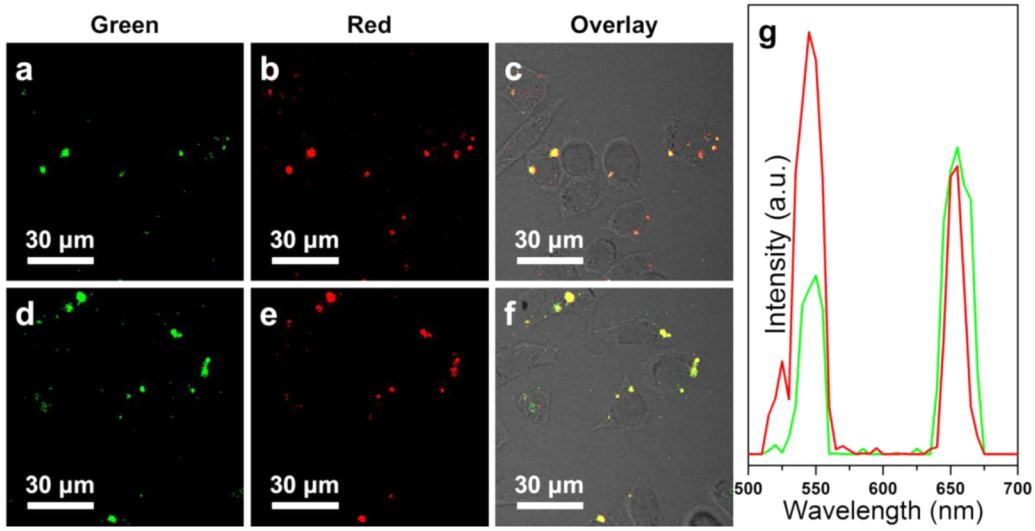

Figure 6. Laser scanning upconversion luminescence images of 42 μg mL^{-1} YSUCNP-ANP (containing 20 μM ANP) incubated withs (a–c) KB cell and (d–f) thiol-eliminated KB cells for 3 h at 37 °C. Emissions was collected from (a, d) 515 to 560 nm (green channel) and (b, e) 635–680 nm (red channel). (g) Detected UCL emission spectra from the KB cells without (green line) and with (red line) pretreatment of NEM (λ_{ex}= 980 nm).

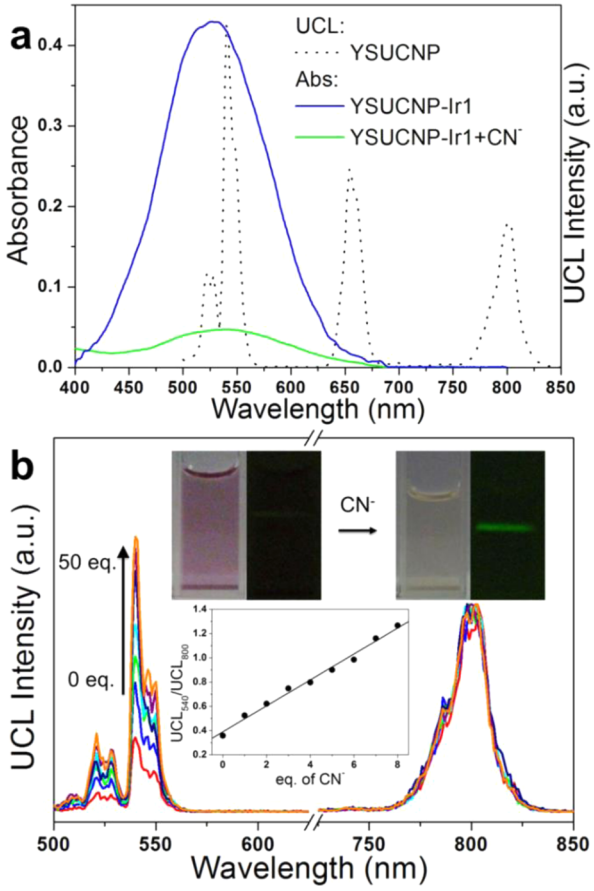

Figure 7. (a) UV–vis absorption spectra of YSUCNP-Ir1 (blue line) and YSUCNP-Ir1 upon addition of CN$^-$ (green line), and the UCL spectrum of YSUCNP (dot line). (b) Changes in UCL spectra and emission photographs (inset up) of 20 μM YSUCNP-Ir1 in PBS (pH 7.5) upon addition of CN$^-$. Inset (down): the linear fitting of UCL_{540}/UCL_{800} in the linearity range.

absorbance at 527 nm[58] and recover the UCL emission. Therefore, CN$^-$ can be detected by the turning-on of the UCL emission of YSUCNP-Ir1.

The titration spectra and digital photographs of YSUCNP-Ir1 added of the CN$^-$ solution are shown in Figure 7b. It can be observed that the green UCL gradually recovered with the addition of CN$^-$. The ratio value of UCL_{540}/UCL_{800} increased linearly when 0–8 equiv. of CN$^-$ was added, and the titration curve reached a saturation point at 8 equiv. (see Figure S2 in the Supporting Information). The calculated detection limit of YSUCNP-Ir1 to CN$^-$ was 6.7 μM, which is one-tenth of the detection limit of a similar UCNP-based LRET nanoprobe we reported using polymer-coating method with the similar complex as chemodosimeter.[59] The upconversion CN$^-$ sensing of YSUCNP-Ir1 was also found to be highly selective (see Figures S3 and S4 in the Supporting Information). Experiments for UCL monitoring of intracellular CN$^-$ was carried out for 48 μg mL^{-1} YSUCNP-Ir1 (containing 10 μM Ir1) to probe the intracellular CN$^-$ in KB cells (see Figure S5 in the Supporting Information).

7. Cytotoxicity of the Upconversion Nanoprobes. The cytotoxicity of YSUCNP-ANP and YSUCNP-Ir1 to the KB cells was further tested using the methylthiazolyldiphenyl-tetrazolium bromide (MTT) method. After addition of 25–400 μg mL^{-1} of YSUCNP-ANP (see Figure S6 in the Supporting Information) and 12.5–200 μg mL^{-1} of YSUCNP-Ir1 (see Figure S7 in the Supporting Information) for 12 h, the cell viability was greater than 85%. Even after 24 h of incubation, cell viability still remained >80%, suggesting low cytotoxicity of the YSUCNP-based nanoprobes.

CONCLUSION

A yolk–shell structured nanoparticle YSUCNP with $NaLuF_4$:Yb,Er,Tm as the inner yolk and porous silica as shell has been synthesized as a general platform to load chromophoric chemodosimeter molecules to construct an upconversion detection nanosystem. The hollow cavity of YSUCNP provides a large cavity to load organic dye probes, and the hydrophilic silica surface endows the nanosystem with surface hydrophilicity to make it workable in a pure water phase. To demonstrate the universality of this approach, a turn-off[60,61] style sensor for Cys/Hcy detection and a turn-on[62,63] style sensor for CN$^-$ detection have been achieved, respectively. The

chemodosimeter-loaded materials exhibit fine cytocompatibility, and can be used for intracellular upconversion detection of the targeted analyte. This protocol based on yolk−shell upconversion nanophosphors loaded with chromophoric chemodosimeters presented provides a general method to prepare similar UC-LRET nanoprobes of special analytes in aqueous solution.

MATERIALS AND METHODS

Materials. 1-Octadecene (ODE, >90%), oleic acid (OA, >90%), and (3-aminopropyl)triethoxysilane (APS, 98%), were purchased from Alfa Aesar. NH_4F, NaOH, acetic acid, tetraethylorthosilicate (TEOS) and sodium dodecylbenzenesulfonate (SDBS) were purchased from Sinopharm. Lauryl sulfonatebetaine (LSB) was purchased from Aladdin chemical company. Rare earth oxides Er_2O_3 (99.999%), Tm_2O_3 (99.999%), Yb_2O_3 (99.999%), and Lu_2O_3 (99.999%) were bought from Shanghai Yuelong New Materials Co. Ltd. The rare earth chlorides were prepared by dissolving the corresponding oxides in concentrated hydrochloric acid (35 wt %). All the chemicals were used without further purification unless otherwise noted. ANP was synthesized according to the previous literature.[47]

Characterization. X-ray diffraction (XRD) patterns were obtained on a Bruker D4 powder X-ray diffractometer using Cu Kα radiation (40 kV, 40 mA). Transmission electron microscopy (TEM) experiments were performed on a JEOL 2011 microscope operated at 200 kV. UV−vis adsorption spectra were recorded on a Shimazu UV 2550 spectrometer. Upconversion luminescence (UCL) spectra were measured on an Edinburgh LFS-920 spectrometer, where an external 0−3 W adjustable continues wavelength (CW) laser at 980 nm (Connet Fiber Optics, China) replaced the xenon lamp as the excitation source. To quantify the weight ratio of UCNPs to silica in the nanoparticles, we treated 16 mg of YSUCNPs with 2 mL of HNO_3, and diluted it with 8 mL of deionized water; the concentrations of the Lu elements in the solution were determined in a Hitachi P-4010 inductively coupled plasma atomic emission spectrometer (ICP-AES).

Synthesis of $NaLuF_4$:20%Yb,1%Er,0.5%Tm Nanocrystals. The β-phase $NaLuF_4$:Yb,Er,Tm nanocrystals was synthesized via a solvothermal method: 0.785 mmol of $LuCl_3$, 0.20 mmol of $YbCl_3$ 0.01 mmol of $ErCl_3$, and 0.005 mmol of $TmCl_3$ were dispersed in 8 mL of oleic acid (OA) and 15 mL of octadecene (ODE), then the mixture was heated to 150 °C for 30 min with a gentle flow of argon gas. After a homogeneous solution was formed, the mixture was cooled to room temperature followed by adding 8 mL methanol solution containing 2.5 mmol NaOH and 4 mmol NH_4F. The temperature was heated to 60 °C to evaporate methanol, then raised to 300 °C in an argon atmosphere for 60 min and cooled to room temperature naturally. The resulting nanoparticles were precipitated by adding ethanol, collecting by centrifugation, and washing with cyclohexane/ethanol (1:1 v/v) three times.

Synthesis of YSUCNPs. Before the synthesis, the OA ligand on the $NaLuF_4$:Yb,Er,Tm surface was removed, 40 mg of $NaLuF_4$:Yb,Er,Tm was dispersed in 6 mL of aqueous solution and the pH was adjust to 2 by adding 0.5 M HCl solution. The ligand-free UCNPs was recuperate by centrifugation, and redispersed in 20 mL of 5 mmol mixed surfactant lauryl sulfonatebetaine/sodium dodecyl benzenesulfonate solution to form a stock solution. Twenty milliliters of the UCNPs stock solution was kept in an oil bath at 40 °C for 30 min, and then 50 μL of triethanolamine, 47 μL of APS, and 300 μL of TEOS were successively added to the resulting solution and stirred for another 1 h. The product was collected by centrifugation, washed with 1:19 (v/v) acetic acid/ethanol solution three times to remove the surfactant, and the obtained product YSUCNPs was kept in ethanol for future applications.

ANP Loading. Five milligrams of ANP was dissolved in 10 mL of ethanol containing 10 mg of YSUCNPs. After being stirred for 12 h, the ANP-loaded YSUCNPs (YSUCNP-ANP) was separated by centrifugation and gently washed with ethanol. The loading ratio of ANP in YSUCNPs measured by UV−vis absorption spectroscopy was 483 μmol g^{-1}.

Ir-1 Loading. Two milligrams of Ir-1 was dissolved in 10 mL of ethanol containing 10 mg of YSUCNPs. After being stirred for 12 h, the Ir-1-loaded YSUCNPs (YSUCNP-Ir-1) was separated by centrifugation and gently washed with ethanol. The loading ratio of Ir-1 in YSUCNPs measured by UV−vis absorption spectroscopy was 208 μmol g^{-1}.

Cell Culture. Human nasopharyngeal epidermal carcinoma cell line (KB cells), was provided by the Institute of Biochemistry and Cell Biology, SIBS, CAS (China). KB cells were grown in RPMI 1640 (Roswell Park Memorial Institute's medium) supplemented with 10% FBS (Fetal Bovine Serum) at 37 °C and 5% CO_2.

Cytotoxicity Assessments. In vitro cytotoxicity was measured by performing MTT assay on KB cells. Cells were seeded into a 96-well cell culture plate at 5×10^4/well, under 100% humidity, and were cultured at 37 °C and 5% CO_2 for 24 h; different concentrations of YSUCNP-ANP or YSUCNP-Ir-1 (0, 25, 50, 100, 200, and 400 μg/mL, diluted in RPMI 1640) were then added to the wells. The cells were subsequently incubated for 12 or 24 h at 37 °C under 5% CO_2. Thereafter, MTT (20 μL; 5 mg/mL) was added to each well and the plate was incubated for an additional 4 h at 37 °C under 5% CO_2. After the addition of 100 μL of DMSO, the assay plate was allowed to stand at room temperature for 2 h. The optical density OD570 value (Abs) of each well with background subtraction at 690 nm, was measured by means of a Tecan Infinite M200 monochromator-based multifunction microplate reader. The following formula was used to calculate the inhibition of cell growth: Cell viability = (mean of Abs. value of treatment group/mean Abs. value of control) × 100%.

YSUCNP-ANP for Intracellular Cys Detection. KB Cells (2×10^8/L) were preseeded on 14 mm glass coverslips and cultured for 24 h to allow adhesion. The cells were incubated with 2 mL of 42 μg mL^{-1} dispersion of YSUCNP-ANP in RPMI 1640 (20 μM for ANP concentration) at 37 °C for 3 h before cell imaging was carried out. For the control group, before the incubation with YSUCNP-AP, the KB cells were initially pretreated with 200 μM thiol-reactive compound N-ethylmaleimide (NEM) at 37 °C for 30 min. Upconversion luminescence imaging was performed on our modified laser scanning upconversion luminescence microscope (LSUCLM) based on an Olympus FluoView FV1000 scan unit with a CW 980 nm laser (Connet Fiber Optics, China) as excitation source. The UCL emission was collected at 515−560 nm and 635−680 nm.

YSUCNP-Ir-1 for Intracellular CN^- Detection. KB Cells (2×10^8/L) were preseeded on 14 mm glass coverslips and cultured for 24 h to allow adhesion. The cells were incubated with 100 μM CN^- for 1 h and washed by PBS solution, and then 2 mL of 48 μg mL^{-1} dispersion of YSUCNP-Ir-1 in RPMI 1640 (10 μM for Ir-1 concentration) was added at 37 °C for 3 h. Upconversion luminescence imaging was carried out on our LSUCLM under excitation at CW 980 nm. The UCL emission was collected at 515−560 nm and 635−680 nm.

ASSOCIATED CONTENT

Supporting Information

(1) Experimental details for the synthesis of chemodosimeter Ir-1, (2) UCL_{540}/UCL_{800} value for YSUCNP-ANP upon addition of different equivalent of Hcy, (3) ratio of UCL intensities at 540 and 800 nm (UCL_{540}/UCL_{800}) for YSUCNP-Ir1 upon addition of different equivalent of CN^-, (4) selectivity studies of YSUCNP-Ir-1, (5) intracellular detection of CN^- using YSUCNP-Ir-1. This material is available free of charge via the Internet at http://pubs.acs.org.

AUTHOR INFORMATION

Corresponding Authors

*E-mail: fengweifd@fudan.edu.cn.
*E-mail: fyli@fudan.edu.cn.

Notes

The authors declare no competing financial interest.

■ ACKNOWLEDGMENTS

This study was financially supported by NSFC (21201038, 21231004, and 21375024), SSTC (11XD1400300, 12ZR1440600, and 13NM1401101), and the State Key Basic Research Program of China (2012CB932403 and 2013CB733700).

■ REFERENCES

(1) Su, Q. Q.; Han, S. Y.; Xie, X. J.; Zhu, H. M.; Chen, H. Y.; Chen, C. K.; Liu, R. S.; Chen, X. Y.; Wang, F.; Liu, X. G. The Effect of Surface Coating on Energy Migration-Mediated Upconversion. *J. Am. Chem. Soc.* **2012**, *134*, 20849−20857.

(2) Liu, Y. S.; Zhou, S. Y.; Tu, D. T.; Chen, Z.; Huang, M. D.; Zhu, H. M.; Ma, E.; Chen, X. Y. Amine-Functionalized Lanthanide-Doped Zirconia Nanoparticles: Optical Spectroscopy, Time-Resolved Fluorescence Resonance Energy Transfer Biodetection, and Targeted Imaging. *J. Am. Chem. Soc.* **2012**, *134*, 15083−15090.

(3) Chen, G. Y.; Ohulchanskyy, T. Y.; Kumar, R.; Agren, H.; Prasad, P. N. Ultrasmall Monodisperse NaYF4:Yb3+/Tm3+ Nanocrystals with Enhanced Near-Infrared to Near-Infrared Upconversion Photoluminescence. *ACS Nano* **2010**, *4*, 3163−3168.

(4) Qiao, X. F.; Zhou, J. C.; Xiao, J. W.; Wang, Y. F.; Sun, L. D.; Yan, C. H. Triple-Functional Core-Shell Structured Upconversion Luminescent Nanoparticles Covalently Grafted with Photosensitizer for Luminescent, Magnetic Resonance Imaging and Photodynamic Therapy In Vitro. *Nanoscale* **2012**, *4*, 4611−4623.

(5) Ostrowski, A. D.; Chan, E. M.; Gargas, D. J.; Katz, E. M.; Han, G.; Schuck, P. J.; Milliron, D. J.; Cohen, B. E. Controlled Synthesis and Single-Particle Imaging of Bright, Sub-10 nm Lanthanide-Doped Upconverting Nanocrystals. *ACS Nano* **2012**, *6*, 2686−2692.

(6) Dou, Q. Q.; Idris, N. M.; Zhang, Y. Sandwich-Structured Upconversion Nanoparticles with Tunable Color for Multiplexed Cell Labeling. *Biomaterials* **2013**, *34*, 1722−1731.

(7) Chen, G. Y.; Shen, J.; Ohulchanskyy, T. Y.; Patel, N. J.; Kutikov, A.; Li, Z. P.; Song, J.; Pandey, R. K.; Agren, H.; Prasad, P. N.; Han, G. alpha-$NaYbF_4$:Tm^{3+})/CaF_2 Core/Shell Nanoparticles with Efficient Near-Infrared to Near-Infrared Upconversion for High-Contrast Deep Tissue Bioimaging. *ACS Nano* **2012**, *6*, 8280−8287.

(8) Shen, J.; Zhao, L.; Han, G. Lanthanide-Doped Upconverting Luminescent Nanoparticle Platforms for Optical Imaging-Guided Drug Delivery and Therapy. *Adv. Drug Delivery Rev.* **2013**, *65*, 744−755.

(9) Park, Y. I.; Kim, J. H.; Lee, K. T.; Jeon, K. S.; Bin Na, H.; Yu, J. H.; Kim, H. M.; Lee, N.; Choi, S. H.; Baik, S. I.; Kim, H.; Park, S. P.; Park, B. J.; Kim, Y. W.; Lee, S. H.; Yoon, S. Y.; Song, I. C.; Moon, W. K.; Suh, Y. D.; Hyeon, T. Nonblinking and Nonbleaching Upconverting Nanoparticles as an Optical Imaging Nanoprobe and T1Magnetic Resonance Imaging Contrast Agent. *Adv. Mater.* **2009**, *21*, 4467−+.

(10) Yu, M. X.; Li, F. Y.; Chen, Z. G.; Hu, H.; Zhan, C.; Yang, H.; Huang, C. H. Laser Scanning Up-Conversion Luminescence Microscopy for Imaging Cells Labeled with Rare-Earth Nanophosphors. *Anal. Chem.* **2009**, *81*, 930−935.

(11) Li, C. X.; Lin, J. Rare Earth Fluoride Nano-/Microcrystals: Synthesis, Surface Modification and Application. *J. Mater. Chem.* **2010**, *20*, 6831−6847.

(12) Wang, G. F.; Peng, Q.; Li, Y. D. Lanthanide-Doped Nanocrystals: Synthesis, Optical-Magnetic Properties, and Applications. *Acc. Chem. Res.* **2011**, *44*, 322−332.

(13) Mader, H. S.; Kele, P.; Saleh, S. M.; Wolfbeis, O. S. Upconverting Luminescent Nanoparticles for Use in Bioconjugation and Bioimaging. *Curr. Opin. Chem. Biol.* **2010**, *14*, 582−596.

(14) Zeng, S. J.; Tsang, M. K.; Chan, C. F.; Wong, K. L.; Hao, J. H. PEG Modified $BaGdF_5$:Yb/Er Nanoprobes for Multi-Modal Upconversion Fluorescent, In Vivo X-ray Computed Tomography and Biomagnetic Imaging. *Biomaterials* **2012**, *33*, 9232−9238.

(15) Dong, H.; Sun, L. D.; Yan, C. H. Basic Understanding of the Lanthanide Related Upconversion Emissions. *Nanoscale* **2013**, *5*, 5703−5714.

(16) Zhou, J.; Liu, Z.; Li, F. Y. Upconversion Nanophosphors for Small-Animal Imaging. *Chem. Soc. Rev.* **2012**, *41*, 1323−1349.

(17) Liu, Q.; Feng, W.; Yang, T.; Yi, T.; Li, F. Upconversion Luminescence Imaging of Cells and Small Animals. *Nat. Protoc.* **2013**, *8*, 2033−2044.

(18) Li, W.; Wang, J.; Ren, J.; Qu, X. Near-Infrared Upconversion Controls Photocaged Cell Adhesion. *J. Am. Chem. Soc.* **2014**, *136*, 2248−2251.

(19) Zheng, W.; Zhou, S. Y.; Chen, Z.; Hu, P.; Liu, Y. S.; Tu, D. T.; Zhu, H. M.; Li, R. F.; Huang, M. D.; Chen, X. Y. Sub-10nm Lanthanide-Doped CaF2 Nanoprobes for Time-Resolved Luminescent Biodetection. *Angew. Chem., Int. Ed.* **2013**, *52*, 6671−6676.

(20) Hao, S. W.; Chen, G. Y.; Yang, C. H. Sensing Using Rare-Earth-Doped Upconversion Nanoparticles. *Theranostics* **2013**, *3*, 331−345.

(21) Vetrone, F.; Naccache, R.; Zamarron, A.; de la Fuente, A. J.; Sanz-Rodriguez, F.; Maestro, L. M.; Rodriguez, E. M.; Jaque, D.; Sole, J. G.; Capobianco, J. A. Temperature Sensing Using Fluorescent Nanothermometers. *ACS Nano* **2010**, *4*, 3254−3258.

(22) Chen, R.; Ta, V. D.; Xiao, F.; Zhang, Q. Y.; Sun, H. D. Multicolor Hybrid Upconversion Nanoparticles and Their Improved Performance as Luminescence Temperature Sensors Due to Energy Transfer. *Small* **2013**, *9*, 1052−1057.

(23) Xie, L. X.; Qin, Y.; Chen, H. Y. Direct Fluorescent Measurement of Blood Potassium with Polymeric Optical Sensors Based on Upconverting Nanomaterials. *Anal. Chem.* **2013**, *85*, 2617−2622.

(24) Tu, N. N.; Wang, L. Y. Surface Plasmon Resonance Enhanced Upconversion Luminescence in Aqueous Media for TNT Selective Detection. *Chem. Commun.* **2013**, *49*, 6319−6321.

(25) Guo, H. C.; Idris, N. M.; Zhang, Y. LRET-Based Biodetection of DNA Release in Live Cells Using Surface-Modified Upconverting Fluorescent Nanoparticles. *Langmuir* **2011**, *27*, 2854−2860.

(26) Jares-Erijman, E. A.; Jovin, T. M. Imaging Molecular Interactions in Living Cells by FRET Microscopy. *Curr. Opin. Chem. Biol.* **2006**, *10*, 409−416.

(27) Wang, Y. H.; Wu, Z. J.; Liu, Z. H. Upconversion Fluorescence Resonance Energy Transfer Biosensor with Aromatic Polymer Nanospheres as the Lable-Free Energy Acceptor. *Anal. Chem.* **2013**, *85*, 258−264.

(28) Wang, L. Y.; Li, Y. D. Green Upconversion Nanocrystals for DNA Detection. *Chem. Commun.* **2006**, 2557−2559.

(29) Liu, J. L.; Cheng, J. T.; Zhang, Y. Upconversion Nanoparticle Based LRET System for Sensitive Detection of MRSA DNA Sequence. *Biosens. Bioelectron.* **2013**, *43*, 252−256.

(30) Wang, Y. H.; Shen, P.; Li, C. Y.; Wang, Y. Y.; Liu, Z. H. Upconversion Fluorescence Resonance Energy Transfer Based Biosensor for Ultrasensitive Detection of Matrix Metalloproteinase-2 in Blood. *Anal. Chem.* **2012**, *84*, 1466−1473.

(31) Wang, L. Y.; Yan, R. X.; Hao, Z. Y.; Wang, L.; Zeng, J. H.; Bao, J.; Wang, X.; Peng, Q.; Li, Y. D. Fluorescence Resonant Energy Transfer Biosensor Based on Upconversion-Luminescent Nanoparticles. *Angew. Chem., Int. Ed.* **2005**, *44*, 6054−6057.

(32) Wang, Y. H.; Bao, L.; Liu, Z. H.; Pang, D. W. Aptamer Biosensor Based on Fluorescence Resonance Energy Transfer from Upconverting Phosphors to Carbon Nanoparticles for Thrombin Detection in Human Plasma. *Anal. Chem.* **2011**, *83*, 8130−8137.

(33) Chen, H. Q.; Yuan, F.; Wang, S. Z.; Xu, J.; Zhang, Y. Y.; Wang, L. Aptamer-Based Sensing for Thrombin in Red Region via Fluorescence Resonant Energy Transfer between NaYF4:Yb,Er Upconversion Nanoparticles and Gold Nanorods. *Biosens. Bioelectron.* **2013**, *48*, 19−25.

(34) Zhang, C. L.; Yuan, Y. X.; Zhang, S. M.; Wang, Y. H.; Liu, Z. H. Biosensing Platform Based on Fluorescence Resonance Energy Transfer from Upconverting Nanocrystals to Graphene Oxide. *Angew. Chem., Int. Ed.* **2011**, *50*, 6851−6854.

(35) Ali, R.; Saleh, S. M.; Meier, R. J.; Azab, H. A.; Abdelgawad, I. I.; Wolfbeis, O. S. Upconverting Nanoparticle Based Optical Sensor for Carbon Dioxide. *Sens. Actuators B* **2010**, *150*, 126−131.
(36) Li, C. X.; Liu, J. L.; Alonso, S.; Li, F. Y.; Zhang, Y. Upconversion Nanoparticles for Sensitive and In-Depth Detection of Cu^{2+} Ions. *Nanoscale* **2012**, *4*, 6065−6071.
(37) Deng, R. R.; Xie, X. J.; Vendrell, M.; Chang, Y. T.; Liu, X. G. Intracellular Glutathione Detection Using MnO_2-Nanosheet-Modified Upconversion Nanoparticles. *J. Am. Chem. Soc.* **2011**, *133*, 20168−20171.
(38) Achatz, D. E.; Meier, R. J.; Fischer, L. H.; Wolfbeis, O. S. Luminescent Sensing of Oxygen Using a Quenchable Probe and Upconverting Nanoparticles. *Angew. Chem., Int. Ed.* **2011**, *50*, 260−263.
(39) Liu, Y.; Chen, M.; Cao, T. Y.; Sun, Y.; Li, C. Y.; Liu, Q.; Yang, T. S.; Yao, L. M.; Feng, W.; Li, F. Y. A Cyanine-Modified Nanosystem for in Vivo Upconversion Luminescence Bioimaging of Methylmercury. *J. Am. Chem. Soc.* **2013**, *135*, 9869−9876.
(40) Seshadri, S.; Beiser, A.; Selhub, J.; Jacques, P. F.; Rosenberg, I. H.; D'Agostino, R. B.; Wilson, P. W. F.; Wolf, P. A. Plasma Homocysteine as a Risk Factor for Dementia and Alzheimer's Disease. *N. Engl. J. Med.* **2002**, *346*, 476−483.
(41) Shahrokhian, S. Lead Phthalocyanine as a Selective Carrier for Preparation of a Cysteine-Selective Electrode. *Anal. Chem.* **2001**, *73*, 5972−5978.
(42) Rusin, O., St; Luce, N. N.; Agbaria, R. A.; Escobedo, J. O.; Jiang, S.; Warner, I. M.; Dawan, F. B.; Lian, K.; Strongin, R. M. Visual Detection of Cysteine and Homocysteine. *J. Am. Chem. Soc.* **2004**, *126*, 438−439.
(43) Tanaka, F.; Mase, N.; Barbas, C. F. Determination of Cysteine Concentration by Fluorescence Increase: Reaction of Cysteine with a Fluorogenic Aldehyde. *Chem. Commun.* **2004**, 1762−1763.
(44) Lee, K. S.; Kim, T. K.; Lee, J. H.; Kim, H. J.; Hong, J. I. Fluorescence Turn-On Probe for Homocysteine and Cysteine in Water. *Chem. Commun.* **2008**, 6173−6175.
(45) Lin, W. Y.; Long, L. L.; Yuan, L.; Cao, Z. M.; Chen, B. B.; Tan, W. A Ratiometric Fluorescent Probe for Cysteine and Homocysteine Displaying a Large Emission Shift. *Org. Lett.* **2008**, *10*, 5577−5580.
(46) Kim, T. K.; Lee, D. N.; Kim, H. J. Highly Selective Fluorescent Sensor for Homocysteine and Cysteine. *Tetrahedron Lett.* **2008**, *49*, 4879−4881.
(47) Zhang, M.; Yu, M. X.; Li, F. Y.; Zhu, M. W.; Li, M. Y.; Gao, Y. H.; Li, L.; Liu, Z. Q.; Zhang, J. P.; Zhang, D. Q. A Highly Selective Fluorescence Turn-On Sensor for Cysteine/Homocysteine and Its Application in Bioimaging. *J. Am. Chem. Soc.* **2007**, *129*, 10322−10323.
(48) Chen, H. L.; Zhao, Q.; Wu, Y. B.; Li, F. Y.; Yang, H.; Yi, T.; Huang, C. H. Selective Phosphorescence Chemosensor for Homocysteine Based on an Iridium(III) Complex. *Inorg. Chem.* **2007**, *46*, 11075−11081.
(49) Li, H. L.; Fan, J. L.; Wang, J. Y.; Tian, M. Z.; Du, J. J.; Sun, S. G.; Sun, P. P.; Peng, X. J. A Fluorescent Chemodosimeter Specific for Cysteine: Effective Discrimination of Cysteine from Homocysteine. *Chem. Commun.* **2009**, 5904−5906.
(50) Ma, Y.; Liu, S.; Yang, H.; Wu, Y.; Yang, C.; Liu, X.; Zhao, Q.; Wu, H.; Liang, J.; Li, F. Y. Water-Soluble Phosphorescent Iridium (III) Complexes as Multicolor Probes for Imaging of Homocysteine and Cysteine in Living Cells. *J. Mater. Chem.* **2011**, *21*, 18974−18982.
(51) Zhou, Y.; Yoon, J. Recent Progress in Fluorescent and Colorimetric Chemosensors for Detection of Amino Acids. *Chem. Soc. Rev.* **2012**, *41*, 52−67.
(52) Jung, H. S.; Chen, X.; Kim, J. S.; Yoon, J. Recent Progress in Luminescent and Colorimetric Chemosensors for Detection of Thiols. *Chem. Soc. Rev.* **2013**, *42*, 6019−6031.
(53) Guo, Z. Q.; Nam, S.; Park, S.; Yoon, J. A Highly Selective Ratiometric Near-Infrared Fluorescent Cyanine Sensor for Cysteine with Remarkable Shift and Its Application in Bioimaging. *Chem. Sci.* **2012**, *3*, 2760−2765.
(54) Liu, J. L.; Liu, Y.; Liu, Q.; Li, C. Y.; Sun, L. N.; Li, F. Y. Iridium(III) Complex-Coated Nanosystem for Ratiometric Upconversion Luminescence Bioimaging of Cyanide Anions. *J. Am. Chem. Soc.* **2011**, *133*, 15276−15279.
(55) Liu, Q.; Peng, J. J.; Sun, L. N.; Li, F. Y. High-Efficiency Upconversion Luminescent Sensing and Bioimaging of Hg(II) by Chromophoric Ruthenium Complex-Assembled Nanophosphors. *ACS Nano* **2011**, *5*, 8040−8048.
(56) Tang, F. Q.; Li, L. L.; Chen, D. Mesoporous Silica Nanoparticles: Synthesis, Biocompatibility and Drug Delivery. *Adv. Mater.* **2012**, *24*, 1504−1534.
(57) Liu, F.; Xiao, Y.; Qian, X.; Zhang, Z.; Cui, J.; Cui, D.; Zhang, R. Versatile Acenaphtho [1, 2-*b*] Pyrrol-Carbonitriles as a New Family of Heterocycles: Diverse S_NAr^H Reactions, Cytotoxicity and Spectral Behavior. *Tetrahedron* **2005**, *61*, 11264−11269.
(58) Lou, B.; Chen, Z.-Q.; Bian, Z.-Q.; Huang, C.-H. Multisignaling Detection of Cyanide Anions Based on an Iridium (iii) Complex: Remarkable Enhancement of Sensitivity by Coordination Effect. *New J. Chem.* **2010**, *34*, 132−136.
(59) Yao, L. M.; Zhou, J.; Liu, J. L.; Feng, W.; Li, F. Y. Iridium-Complex-Modified Upconversion Nanophosphors for Effective LRET Detection of Cyanide Anions in Pure Water. *Adv. Funct. Mater.* **2012**, *22*, 2667−2672.
(60) Kuang, H.; Chen, W.; Xu, D. H.; Xu, L. G.; Zhu, Y. Y.; Liu, L. Q.; Chu, H. Q.; Peng, C. F.; Xu, C. L.; Zhu, S. F. Fabricated Aptamer-Based Electrochemical "Signal-Off" Sensor of Ochratoxin A. *Biosens. Bioelectron.* **2010**, *26*, 710−716.
(61) Yu, H. B.; Fu, M. Y.; Xiao, Y. Switching Off FRET by Analyte-Induced Decomposition of Squaraine Energy Acceptor: A Concept to Transform "Turn Off" Chemodosimeter into Ratiometric Sensors. *Phys. Chem. Chem. Phys.* **2010**, *12*, 7386−7391.
(62) Leung, K. H.; He, H. Z.; Ma, V. P. Y.; Chan, D. S. H.; Leung, C. H.; Ma, D. L. A Luminescent G-Quadruplex Switch-On Probe for the Highly Selective and Tunable Detection of Cysteine and Glutathione. *Chem. Commun.* **2013**, *49*, 771−773.
(63) He, H. Z.; Chan, D. S. H.; Leung, C. H.; Ma, D. L. A Highly Selective G-quadruplex-Based Luminescent Switch-On Probe for the Detection of Gene Deletion. *Chem. Commun.* **2012**, *48*, 9462−9464.